Experimental Aerodynamic Characteristics of an NACA 0012 Airfoil with Simulated Ice

K. D. Korkan,* E. J. Cross Jr.,† and C. C. Cornell‡
Texas A&M University, College Station, Texas

An experimental program was conducted with an NACA 0012 airfoil to investigate the effect of Reynolds number on the aerodynamic coefficients with and without a leading-edge simulated ice shape. Six Reynolds numbers from 0.36 to 3.36×10^6 were investigated at both positive and negative angles of attack through stall. Values of ΔC_d, ΔC_ℓ, $\Delta C_{\ell_{max}}$, and $\Delta C_{m_{c/4}}$ were measured for the no-ice/generic-ice airfoil configurations. The experimental values have shown that the addition of the generic ice shape causes premature stall with a considerable reduction in $C_{\ell_{max}}$ and stall angle of attack; an increase in the drag values of 120-200% compared to the clean airfoil values; and a significant increase in $C_{m_{c/4}}$ resulting in positive values of dC_m/dC_ℓ. However, the aerodynamic coefficients of the airfoil with the leading-edge simulated ice showed little dependence on Reynolds number throughout the range tested, unlike that of the clean airfoil configuration.

Nomenclature

c	= airfoil chord
C_d	= drag coefficient, $D/q_\infty c$
C_{d_0}	= drag coefficient at 0-deg angle of attack
C_ℓ	= lift coefficient, $L/q_\infty c$
$C_{\ell_{max}}$	= maximum lift coefficient
$C_{m_{c/4}}$	= moment coefficient, $M/q_\infty c^2$, at $c/4$
D	= drag force
k	= grit diameter
L	= lift force
M	= pitching moment
q	= dynamic pressure, $\rho_\infty V_\infty^2/2$
Re_∞	= Reynolds number, $\rho_\infty V_\infty c/\mu_\infty$
V_∞	= freestream velocity
α	= airfoil angle of attack
α_{L_0}	= airfoil angle of attack at zero lift
μ_∞	= air viscosity
ρ	= air density

Introduction

THE accretion of ice on airfoil surfaces has been a significant factor in limiting the safe flight regimes of various aircraft due to performance degradation. In the case of rotating systems such as propellers and helicopter rotor blades, drastic reductions in performance have been experienced with respect to thrust and power required when ice is allowed to accrete. Analytical models which provide theoretical values of performance degradation due to an icing encounter on helicopter main rotor blades in hover[1] and in forward flight[2] in addition to a propeller[3] have been under study. As noted in these previous studies, there is a paucity of data regarding the change in the aerodynamic coefficients when an ice shape is added to the leading edge of an airfoil. Since the current theoretical models employ airfoil data banks, it is imperative that the incremental change of C_ℓ, C_d, $C_{\ell_{max}}$, and $C_{m_{c/4}}$ due to ice accretion be known to further enhance the current theoretical efforts. Further, since these data are to be employed in the investigation of an experimental and theoretical study of the performance degradation of a model helicopter main rotor with simulated ice shapes,[4,5] the effects of Reynolds number are of paramount interest, in addition to the use and validity of generic ice.

The series of tests described in this paper were undertaken to determine the effect of Reynolds number on the aerodynamic performance of the airfoil with and without generic ice addition. Previous studies have taken a similar approach. For example, Brumby[6] tabulated data on the effect of airfoil surface roughness on maximum lift coefficient, and Bragg and Gregorek[7] have used simulated rime ice on the leading edge of an NACA 65A413 airfoil. Unlike the previous studies, with the exception of Bragg and Gregorek,[7] this series of tests measures the effect of the generic ice on airfoil lift, drag, and pitching moment and thereby provides a convenient data bank which can be used in helicopter theoretical prediction studies in comparison with experiment.[4,5]

NACA 0012 Airfoil Experiment

Wind tunnel tests were conducted with a two-dimensional NACA 0012 airfoil having a 21-in. chord to investigate the effect of Reynolds number on the aerodynamic performance with and without a generic ice shape attached to the airfoil leading edge. The Reynolds number range investigated consisted of 0.36 to 3.36×10^6 which includes the operating regime of a model helicopter rotor tip.[4,5] The airfoil experiment also served to generate a data bank for the generic ice shape addition including roughness in terms of ΔC_d, ΔC_ℓ, $\Delta C_{\ell_{max}}$, and $\Delta C_{m_{c/4}}$.

Experimental Facilities

The airfoil tests utilized the Texas A&M University 7×10 ft low-speed wind tunnel. The closed-circuit tunnel has a test section 7 ft high, 10 ft wide, and 12 ft long, fabricated of structural steel, and lined with solid marine plywood and plexiglass. Any desired test section Reynolds number up to 1.84×10^6/ft may be obtained by proper blade pitch angle positioning of the 12.5-ft diam, four-blade Curtiss Electric propeller, as shown in Fig. 1.

Presented as Paper 84-0184 at the AIAA 22nd Aerospace Sciences Meeting, Reno, Nev., Jan. 9-12, 1984; received April 3, 1984; revision received Sept. 10, 1984.

*Associate Professor, Aerospace Engineering Department. Associate Fellow AIAA.

†Professor/Head, Aerospace Engineering Department. Associate Fellow AIAA.

‡Graduate Research Assistant. Student Member AIAA.

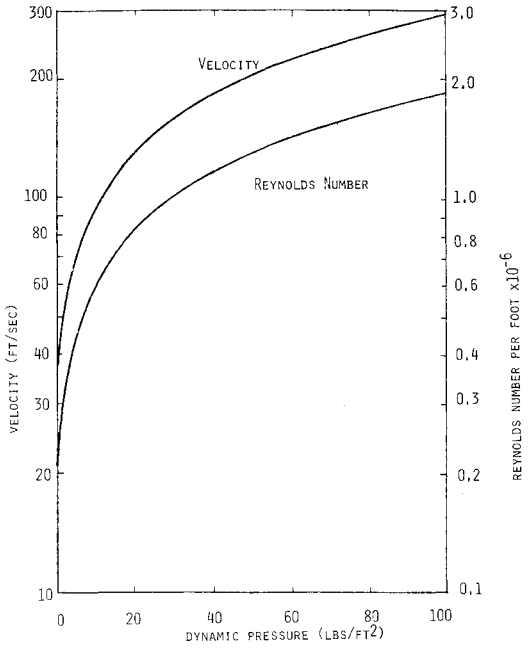

Fig. 1 Wind tunnel test section velocity and Reynolds number at standard conditions.

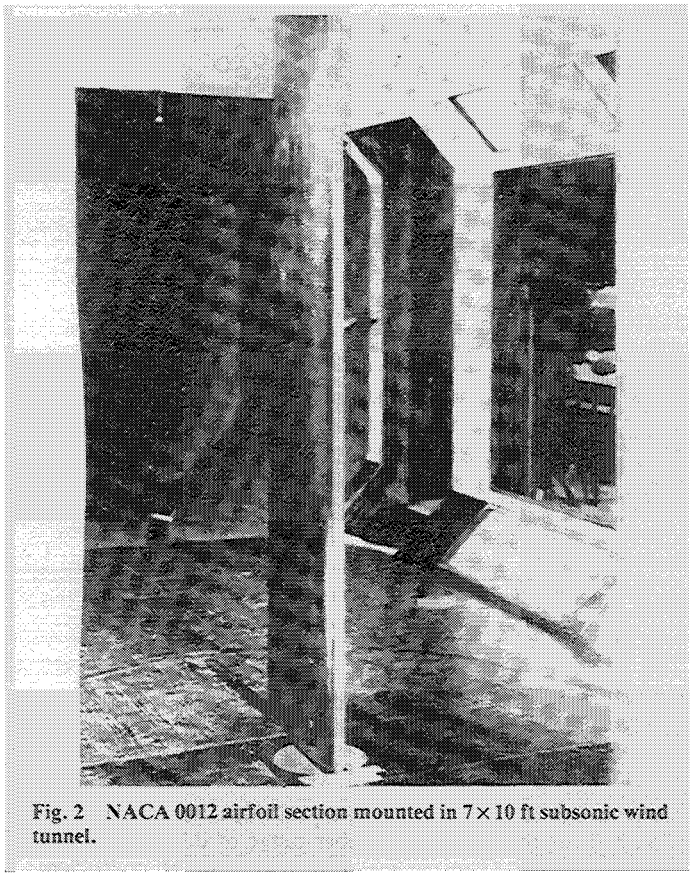

Fig. 2 NACA 0012 airfoil section mounted in 7 × 10 ft subsonic wind tunnel.

Lift, drag, and moment measurements are taken via the facility's six component external balance. Resolution of forces and moments is accurate to within ±0.1 lb and ±0.1 ft-lb, respectively.[8] Upon transmission of the measurements to the Perkin-Elmer 8/16 E data acquisition and analysis computer system, corrections are included for wind tunnel interference and model support effects. On-line plotting capabilities of a Hewlett-Packard 7021-T Plotter enable C_ℓ vs α, C_d vs C_ℓ, and $C_{m_{c/4}}$ vs C_ℓ plots to be obtained for detailed examination.

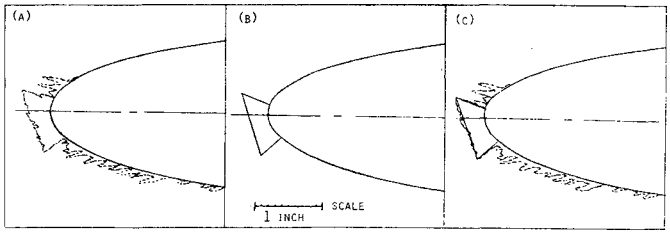

Fig. 3 a) Actual ice accretion as documented during flight tests of UH-1H helicopter. b) Ice shape used on tunnel model (less roughness). c) Comparison of a and b.[10]

NACA 0012 Airfoil Model

A 21-in.-chord NACA 0012 airfoil section was mounted vertically in the test section, cantilevered to the external balance beneath the wind tunnel floor, and pivoted at the wind tunnel ceiling as shown in Fig. 2. Clearances of less than 0.25 in. were maintained between the model, tunnel floor, and ceiling panels. Three-dimensional effects are minimal in these regions due to test section boundary-layer thickness.[9]

The generic ice shape utilized during the present tests has been documented by The Ohio State University Aeronautical and Astronautical Research Laboratory (OSU/AARL) on the main rotor of a UH-1H helicopter during a recent icing flight test program.[10] The main rotor of this configuration employs an NACA 0012 airfoil with a 21-in. chord. Although several shapes were identified as a function of radial location on the main rotor during this flight test program, the ice profile chosen for this study was based on the criteria that the profile could be reasonably scaled to the model helicopter main rotor including roughness.[4,5] The 44% radial station of the UH-1H main rotor was selected for a flight test condition of a 3-min icing encounter with a free air temperature of −19 deg F and a liquid water content of 0.7 g/m^3. Figure 3 shows a projection of the ice shape as molded during the OSU/AARL flight tests and that used on the tunnel airfoil model. It may be noted that an accurate reproduction of the flight test shape may not be required since one of the objectives is to validate scale testing as noted by previous studies,[7] and thereby justifies the exclusion of the ice feathers on the upper and lower surfaces of the airfoil.

A molding technique was selected in fabricating the simulated ice shape. To insure maximum surface contact between the airfoil leading edge and the matching contour of the generic ice shape, the airfoil section was used in the molding process. With the tunnel airfoil model positioned horizontally, a channel was formed on the leading edge by spanning the airfoil with two strips of aluminum. L-shape bends were pressed into these aluminum mold walls to provide stiffness and ensure the appropriate ice depth. End-plate templates were secured to both ends of the airfoil section to orient the mold channel with respect to the airfoil leading edge. Finally, spanwise consistency of the mold was checked with a template insert and maintained with several outriggers. Upon application of a mold releasing agent, fiberglass resin with a hardening catalyst was poured into the channel and reinforced with fiberglass cloth. Minor hand finishing, using templates as checks, provided a consistent, representative ice shape. Holes were then drilled and tapped through the generic ice shape into the airfoil leading edge to insure secure and correct positioning during the wind tunnel tests.

Roughness was added to the generic ice shape to simulate actual ice roughness. As noted by earlier studies,[11] a typical ice roughness of $k/c = 0.001$ was chosen. An aluminum oxide grit with an average size of 0.028 in. was selected to yield a k/c value of 0.0013 on the 21-in.-chord airfoil model. The grit was applied to the generic ice shape by coating the surface with 3-M spray adhesive and applying the grain material. Two successive coats of the adhesive were then applied to secure

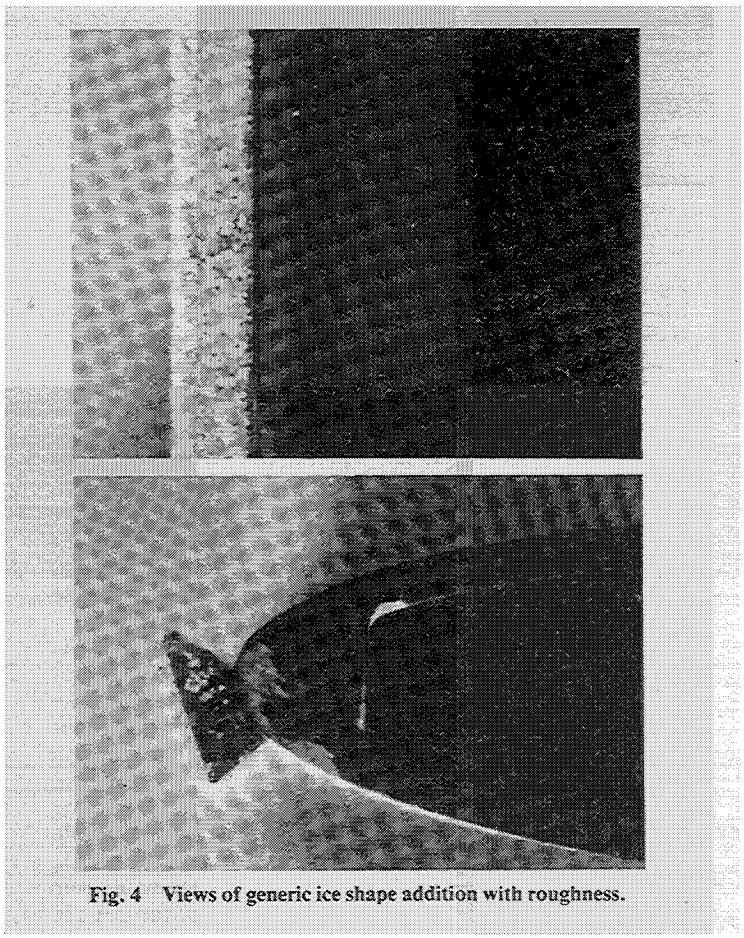

Fig. 4 Views of generic ice shape addition with roughness.

the particles and provide a realistic roughness surface as shown in Fig. 4.

NACA 0012 Airfoil Aerodynamic Performance

The NACA 0012 airfoil section was initially tested with no generic ice addition to obtain baseline data and establish agreement with Abbott and Von Doenhoff[12] for the case of $Re = 3.3 \times 10^6$. The generic ice shape was then attached to the leading edge of the airfoil and the test matrix was repeated. Effects on the lift, drag, and pitching moment about the quarter-chord as a function of angle of attack and Reynolds number were then examined to determine aerodynamic increments due to the addition of the generic ice shape.

Lift

The addition of the asymmetric generic ice shape with roughness to the leading edge of the NACA 0012 airfoil, in comparison to the clean airfoil, is expected to cause early boundary-layer transition in addition to leading-edge separation and reattachment. As shown in Fig. 5 for a Reynolds number of 1.4×10^6, the addition of the generic ice shape does cause premature stall with a significant reduction in $C_{\ell_{max}}$ and stall angle of attack. Here it can also be seen that because of the asymmetric location of the generic ice shape on the airfoil leading edge, the maximum lift coefficient and corresponding angle of attack for both positive and negative values differ unlike that of the symmetrical airfoil. For example, a $C_{\ell_{max}}$ of 0.99 is measured at an α of 12.2 deg as opposed to a $C_{\ell_{max}}$ of 0.86 at an α of -10.5 deg. Also due to the asymmetry of the ice addition, resulting in leading-edge boundary-layer separation and distortion of the airfoil pressure distribution, camber is introduced resulting in a zero lift angle of attack shift of approximately -0.5 deg. This appears to be consistent at all Reynolds numbers tested as shown in Fig. 6. Also shown in this figure, it can be seen that

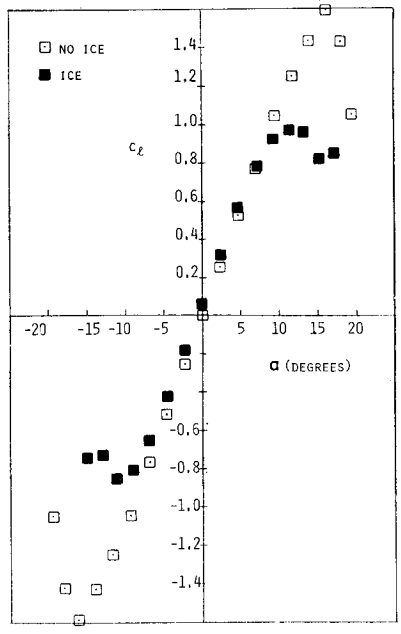

Fig. 5 Experimental C_ℓ-α data for an NACA 0012 airfoil clean and with simulated leading-edge ice ($Re = 1.4 \times 10^6$).

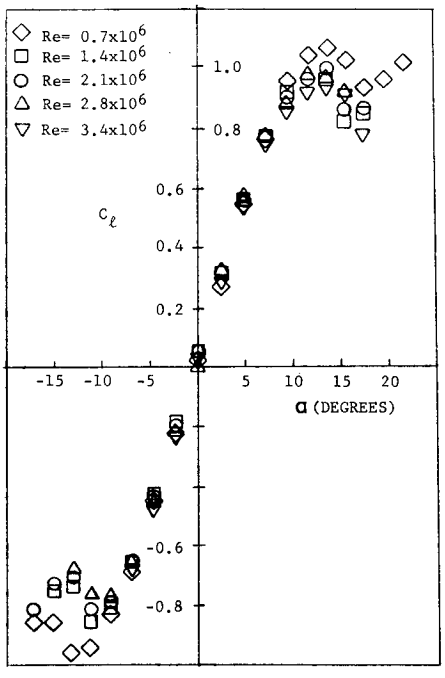

Fig. 6 Reynolds number effects on the lifting performance of the NACA 0012 airfoil with simulated ice.

there is no change in the lift-curve slope which could be detected for the Reynolds number range of 0.7 to 3.4×10^6. However, a slight dependence of the maximum lift coefficient on Reynolds number is indicated as shown in Fig. 7 in comparison to the clean or no-ice two-dimensional airfoil values. With regard to the increase in $C_{\ell_{max}}$ with decreased Reynolds number, it has been suggested that this phenomenon is related to the combined excessive leading- and trailing-edge boundary-layer separation resulting in a $C_{\ell_{max}}$ that is relatively insensitive to Reynolds number.

The anticipated leading-edge boundary-layer separation and reattachment eventually leads to premature stall as shown in Fig. 5. However, in the vicinity of the maximum lift coefficient, the reattachment of the boundary layer after stall

has also been encountered, as shown in Fig. 8 for a Reynolds number of 0.7×10^6. This phenomenon is significant enough to cause the lift of the clean and generic ice airfoil to coincide at an angle of attack of approximately 20 deg for this Reynolds number.

Drag

The increase in the drag values for the airfoil with generic ice attached for a Reynolds number of 2.1×10^6 is shown in Fig. 9. Here, upon comparison with the clean airfoil, it can be seen that an increase of approximately 120% is found for C_{d_0}. The ΔC_d values increase significantly as C_ℓ increases, e.g., exceeding 200% at a C_ℓ of 0.6. For negative angles of attack, due to the asymmetry of the generic ice shape, the ΔC_d exceeds this value (Fig. 9). Reynolds number effects, shown in Fig. 10, indicate a slight dependence for the range of 1.4 to 2.8×10^6 with an increase for a Reynolds number of 3.4×10^6 for both positive and negative angles of attack. The magnitude of the ΔC_d is of the same order as that predicted by Bragg and Gregorek[7] and Lee.[10]

Pitching Moment

Moment coefficients about the airfoil quarter-chord were also measured, and a representative comparison of the clean and generic ice cases is presented in Fig. 11 for a Reynolds number of 2.1×10^6. The moment coefficient data for the clean configuration are characteristic of the symmetric airfoil and are agreeable within the resolution of the wind tunnel balance. The addition of the generic ice shape results in two effects on the pitching moment variation as a function of C_ℓ. A small nose-down pitching moment caused by the camber effect similar to the α_{L_0} shift was noted. Also, the influence of

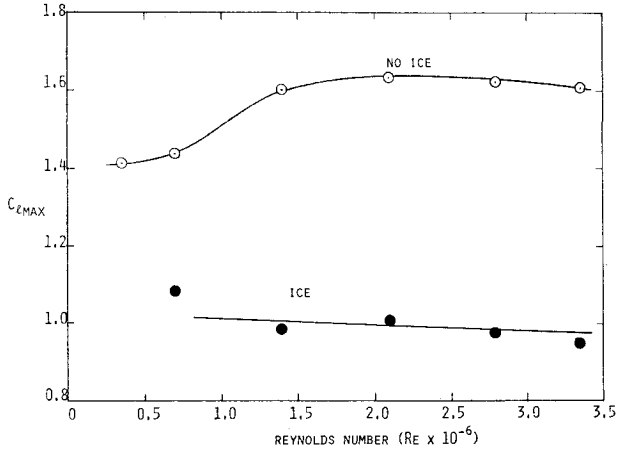

Fig. 7 Variation of maximum lift coefficient with Reynolds number of the NACA 0012 airfoil clean and with simulated ice.

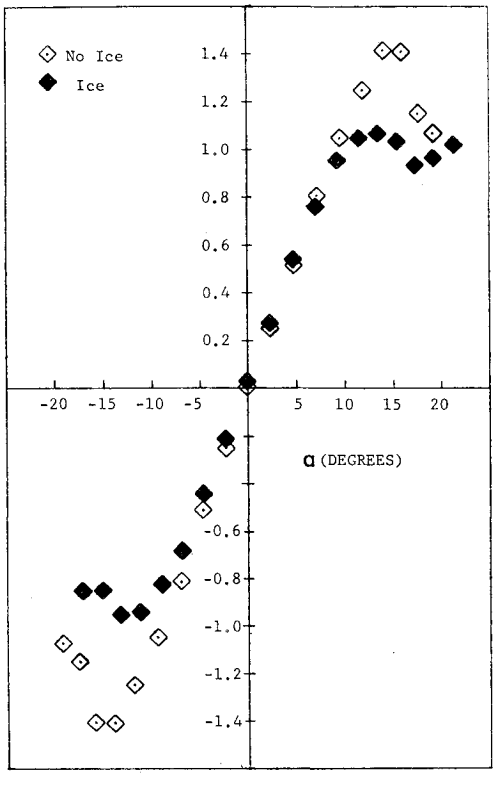

Fig. 8 Experimental C_ℓ-α data of an NACA 0012 airfoil clean and with simulated leading-edge ice ($Re=0.7\times10^6$).

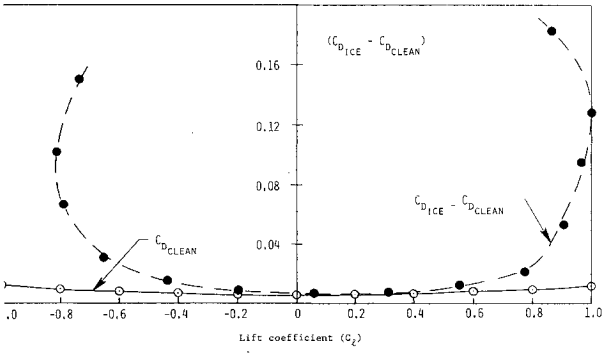

Fig. 9 Wind tunnel measurements of the increase in drag, ΔC_d, due to simulated ice on an NACA 0012 airfoil ($Re=2.1\times10^6$).

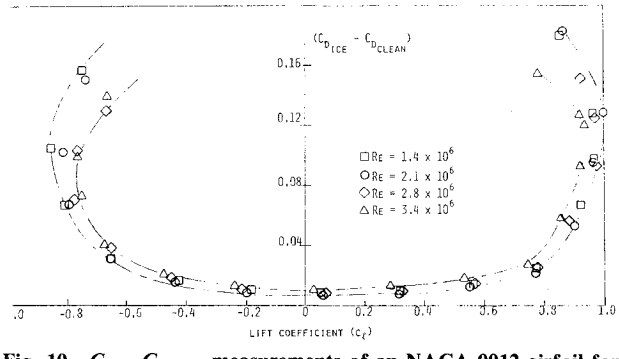

Fig. 10 $C_{d_{ice}}$-$C_{d_{clean}}$ measurements of an NACA 0012 airfoil for a Reynolds number range 1.4-3.4$\times10^6$.

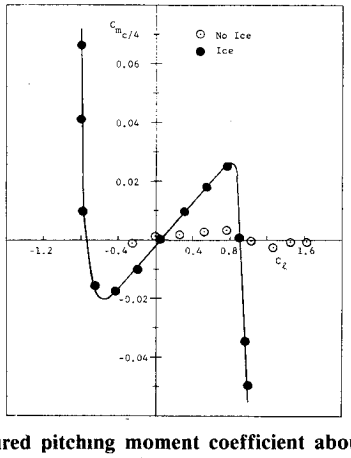

Fig. 11 Measured pitching moment coefficient about the quarter-chord of an NACA 0012 airfoil clean and with simulated ice ($Re=2.1\times10^6$).

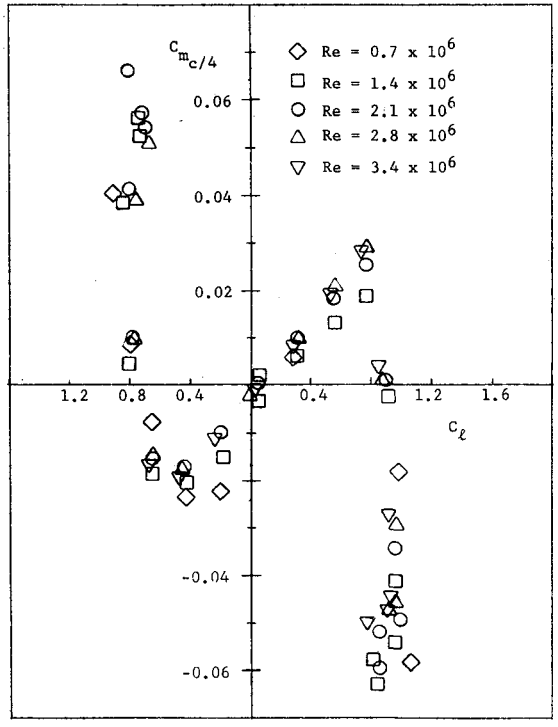

Fig. 12 Effects of Reynolds number on pitching moment measurement of an NACA 0012 airfoil with simulated ice.

the simulated ice on dC_m/dC_ℓ is large, where the slope of the curve becomes positive due to the region of incipient separation and its influence on the airfoil pressure distribution as a result of the artificial introduction of camber by the generic ice shape. This effect appears to be relatively independent of Reynolds number for the range tested as shown in Fig. 12.

Summary

In support of model helicopter tests,[4,5] wind tunnel tests were conducted with a two-dimensional NACA 0012 airfoil having a 21-in. chord to investigate the effect of Reynolds number on the aerodynamic performance with and without a generic ice shape attached to the airfoil leading edge. The Reynolds number range investigated consisted of 0.36 to 3.36×10^6 which includes the operating regime of the model helicopter rotor tip.[4,5] Values of ΔC_d, ΔC_ℓ, $\Delta C_{\ell_{max}}$, and $\Delta C_{m_{c/4}}$ were presented for the no-ice/generic-ice airfoil configurations, and have shown that the addition of simulated ice to the leading edge of the airfoil creates premature stall with a considerable reduction in $C_{\ell_{max}}$ and stall angle of attack. An increase in the drag values of 120-200% compared to the clean airfoil values was measured in addition to a significant increase in the airfoil moment coefficient about the quarter-chord resulting in positive values of dC_m/dC_ℓ. The aerodynamic coefficients of the airfoil with the leading-edge generic ice showed little dependence on the Reynolds number range tested.

Acknowledgments

This work was supported in part by NASA Lewis Research Center Grant NAG 3-242, "Propeller/Rotor Icing Study." The authors also wish to thank Dr. R. J. Shaw of NASA Lewis Research Center for his advice and continued support of our icing research efforts, and the Texas A&M University Subsonic Wind Tunnel Group for their participation and excellent cooperation in the tests documented in this paper.

References

[1]Korkan, K. D., Dadone, L., and Shaw, R. J., "Helicopter Rotor Performance Degradation in Natural Ice Encounter," *Journal of Aircraft*, Vol. 21, Jan. 1984, pp. 84-85.

[2]Korkan, K. D., Shaw, R. J., and Dadone, L., "Performance Degradation of Helicopter Rotor Systems in Forward Flight Due to Rime Ice Accretion," AIAA Paper 83-0029, Jan. 1983.

[3]Korkan, K. D., Dadone, L., and Shaw, R. J., "Performance Degradation of Propeller Systems Due to Rime Ice Accretion," *Journal of Aircraft*, Vol. 21, Jan. 1984, pp. 44-49.

[4]Korkan, K. D., Cross, E. J. Jr., and Cornell, C. C., "Experimental Study of Performance Degradation of a Model Helicopter Main Rotor with Simulated Ice Shapes," AIAA Paper 84-0184, Jan. 1984.

[5]Korkan, K. D., Cross, E. J. Jr., and Miller, T. L., "Performance Degradation of a Helicopter Main Rotor in Hover and Forward Flight with a Generic Ice Shape," AIAA 13th Aerodynamic Testing Conference, March 1984. AIAA Paper 84-0609.

[6]Brumby, R. E., "Wing Surface Roughness, Cause and Effect," *DC Flight Approach,* Jan. 1979, pp. 2-7.

[7]Bragg, M. B. and Gregorek, G. M., "Aerodynamic Characteristics of Airfoils with Ice Accretions," AIAA Paper 82-0282, Jan. 1982.

[8]"Low Speed Wind Tunnel Facility Handbook," Texas Engineering Experiment Station, Texas A&M University, College Station, Tex., 1982.

[9]Nicks, O. and Ferrell, W., "Boundary Layer Profile Measurements on the Floor of the 7' × 10' Low Speed Wind Tunnel," Texas Engineering Experiment Station, Texas A&M University, College Station, Tex., Rept. TR 8130, Jan. 1982.

[10]Lee, J. D., "Aerodynamic Evaluation of a Helicopter Rotor Blade with Ice Accretion in Hover," AIAA Paper 84-0608, March 1984.

[11]Bragg, M. B., "Rime Ice Accretion and its Effect on Airfoil Performance," NASA CR 165599, March 1982.

[12]Abbott, I. H. and Von Doenhoff, A. E., *Theory of Wing Sections*, Dover Publications, New York, 1959.